Funicularity of conics

Xavier Tellier, Cyril Douthe, Laurent Hauswirth, Olivier Baverel

Funicularity of conics

Xavier TELLIER* [a b], Cyril DOUTHE[a], Laurent HAUSWIRTH[b], Olivier BAVEREL[a c]
* [a] Laboratoire Navier, Ecole des Ponts, CNRS, Université Gustave Eiffel
77455 Champs-sur-Marne - France
xavier.tellier@enpc.fr
[b] Laboratoire d'Analyse et de Mathématiques Appliquées, UGE, UPEC, CNRS, Champs-sur-Marne, France
[c] GSA / ENS Architecture Grenoble, France

Abstract

Funicular structures can resist a given load with pure axial forces, and therefore tend to use material very efficiently. One main challenge in their design is the form-finding, which often requires advanced numerical methods. In this article, we show analytically that a very common family of curves, conics, is funicular for a particular load case: a uniform radial load emanating from a focus (Figure 1). The result is a generalization of the well-known funicularity of parabolas and arcs of circles, respectively under uniform vertical load and constant normal pressure. It can be used to design self-stressed structures by hand without the need for calculations. Portions of conics can be combined to obtain original shapes.

Keywords: Funicular structures, conics, self-stressed structures, tensegrity, spoke wheel

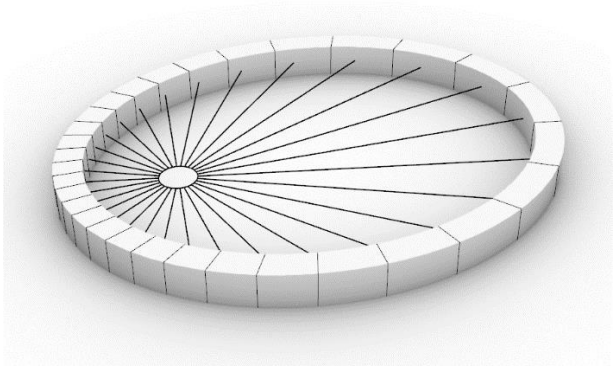

Figure 1: An elliptical arch tensioned by radial cables emanating from a focal point, with constant cable tension and constant angle between cables, is funicular.

1. Introduction

Funicular structures have been abundantly researched since the XVIII[th] century and Hook's hanging chain. As they are able to resist a given load without bending or shear, they tend to use less material, thus minimizing cost and embodied energy. With materials such as masonry or cables, funicularity is necessary due to the low bending resistance.

Funicular curves

Even though the research on funicular structures focuses nowadays on structures with complex connectivity (Lee *et al.* 2015; Ohlbrock and Schwartz 2016), or complex geometry such as shells (Block 2009; Vouga *et al.* 2012; Liu *et al.* 2013; Tellier *et al.* 2018, 2020), a historical problem has been the design of funicular line elements. This question is of particular importance for the design of suspension cables and masonry arches (Heyman 1997). The most common method to draw funicular curves for a

particular load configuration is graphic statics, using the reciprocal force diagram (Cremona 1890). This method can be done by hand drawing or by scripting a parametric CAD software, and is still commonly used to teach structures in architecture schools.

Analytical funicular curves are widely used by designers, especially in conceptual design phases. The most well-known examples are the circles, parabolas and catenaries, which are respectively funicular for a uniform normal pressure, a constant vertical load, and self-weight (in the case of a constant section). These primitives sometimes serve directly as the geometry of the final structure. For example, the Gateway arch in Saint Louis, Missouri, is a modified catenary, and the arch of the Bixby Creek Bridge in California is a parabola (Figure 3). These primitives are however also often used as mechanical models. For example, it is common to approximate arches and sagging cables as parabolas to estimate internal forces.

Analytical funicular curves can be found for a wide variety of loading configurations, beyond the ones of the circles, parabola and catenary. (Dennis 1994) shows that these three curves are solutions of a same one-parameter family of differential equations. By varying this parameter, he obtains a new curve which is funicular for a peculiar load case. Funicular curves for hydrostatic pressure were investigated in (Gavin and Reilly 2000; Wang and Wang 2002; Fung 2003), a potential application being section design for a tunnel lying on the seabed. (Wang and Wang 2015) considered a superposition of a uniform vertical load with self-weight. The shape of a cable dragged by two boats and subject only to viscous forces was found in (Simpson and Tabarrok 1976) to be a catenary. (Hill *et al.* 1979) derived the shape of an arch which is funicular under self-weight and with constant axial stresses: the solution has varying section depth, and is therefore not a catenary.

Self-stressed structures

Funicular structures are often lightweight. As a consequence, their dead load is in general not dominant in comparison to live loads, including in particular wind suction and asymmetrical load scenarios. A common solution to maintain stability under such conditions is prestressing. In structures such as cable nets or membranes, prestressing is also necessary to obtain sufficient stiffness. This is particularly true for tensegrity structures, which are especially effective for long span envelopes. A notable example is the 185m-wide roof of the Georgia dome in Atlanta (Figure 2), built in 1992, or the more recent Bao'an stadium in Shenzen.

(Todisco and Corres 2018) highlight another potential use for self-stressing in arches. For architectural purposes, the shape of an arch might not be funicular under self-weight. The traditional solution is then to resort to bending resistant systems. However, if external loads are added to the arch, a pure compression state can be achieved, such that it can be built in masonry. A famous example is the Pavilion of the Future at the 1992 Sevilla Expo, designed by Peter Rice (Figure 2, right): Circular arches, which are not funicular under self-weight, have been made funicular by superimposing a state of self-stress.

Form-finding of self-stressed structures is challenging as the load path is not linear anymore. Numerical tools such as force density (Schek 1974) or dynamic relaxation (Otter *et al.* 1966) are often required. However, analytical models are also commonly used at conceptual design stages. One common analytical model is the spoke-wheel diaphragms: circular arches can be prestressed funicularly by radial spokes with constant tension. Such a system is used notably to brace the gridshell of the Hamburg history museum (Schober 2015). A graphical construction method to obtain other shapes than circles in a spoke-wheel structure is proposed in (Tamai 2019).

Figure 2: Self-stressed structures. Left: Pavilion of the Future at the 1992 Sevilla Expo. Right: Georgia dome

Conics

Circles and parabolas, discussed earlier, are special types of conics: they correspond to sections of cones by planes. Conics are commonly used in design. For example, Paris subways stations have an elliptical cross section. Ellipses can be constructed geometrically with a pen and a piece of rope, a property which was highly valuable before the advent of digital tools. They are however still used today, for example in the geometry of the beams of the Hangar-7 in Salzburg (Figure 3). The minimum thickness of an elliptical masonry arch subject to self-weight is studied in (Alexakis and Makris 2013). Ellipses can also be obtained by applying an affine transformation to a circle. As affine transformations transform a self-stressed geometry into another self-stressed geometry (Rankine 1858), one simple way to obtain a self-stressed elliptical arch is to apply an affine transformation to a circular spoke-wheel (i.e. applying a "1D-scaling"). More generally, any projective transformation of a funicular structure conserves its equilibrium, a point that was recently explored for design applications in (Fivet 2016). Applying such deformations to spoke-wheels, one obtains an elliptical wheel in which spokes converge to a point which is not the ellipse centroid.

Hyperbolas also often appear in double-curvature structures. They are the cross sections of hyperboloids of revolution, such as the Water Tank in Novgorod (Figure 3), which popularity is due to the fact that they can be built from straight beams.

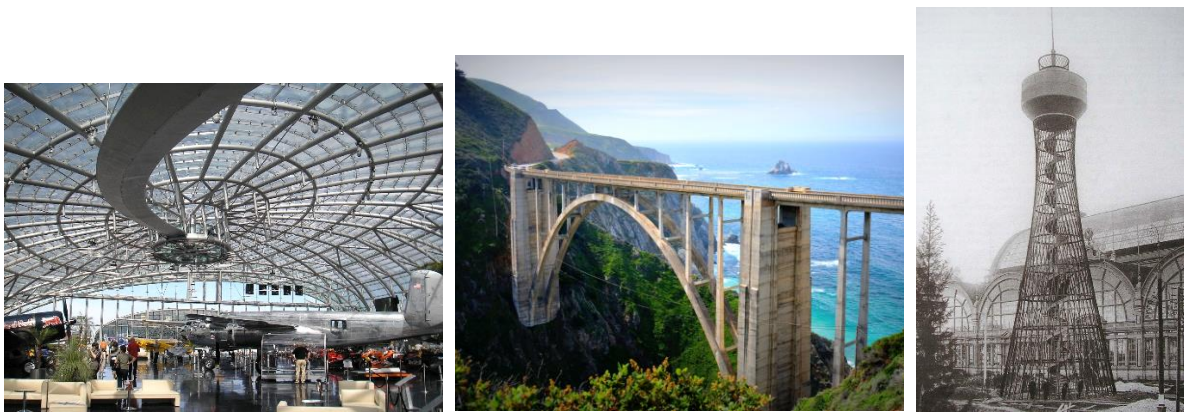

Figure 3: Examples of conics in architecture, respectively ellipses, parabola, and hyperbolas
Left: Hangar-7, Salzburg (tilted ellipsoid) (©F412)
Middle: Bixby Creek Bridge, California (©Reverie Rambler)
Right: Water Tank in Novgorod by Vladimir Shokhov

Contributions

Section 2 of this paper shows how the well-known funicularity of circles and parabolas can be generalized to any conic. This funicularity is obtained for a particular load, called a uniform radial load. Axial forces can be obtained from a simple analytical formula. Section 3 shows how this result can be applied to discrete conics, with a direct application to cable fan diaphragms. Section 4 demonstrates how these

results can be used for the conceptual design of self-stressed structures. Finally, section 5 discusses the limitations and potential future work.

2. Funicularity

2.1 Geometry of conics

In this section, we briefly review the geometry of conics. A thorough exploration of conics properties can be found for example in (Glaeser *et al.* 2016). As illustrated in Figure 4, a conic can be parametrized in polar coordinates as follows:

$$r(\theta) = \frac{p}{1 + e\cos\theta} \tag{1}$$

Where:

- The point $r = 0$ is a focus of the conic;
- p is the distance between this focus and the point at angle $\pi/2$: $p = r(\pi/2)$;
- e is the eccentricity. Its value determines the type of the conic. More precisely, the conic is:
  - A circle if $e = 0$;
  - An ellipse if $0 < e < 1$;
  - A parabola if $e = 1$;
  - A hyperbola if $e > 1$.

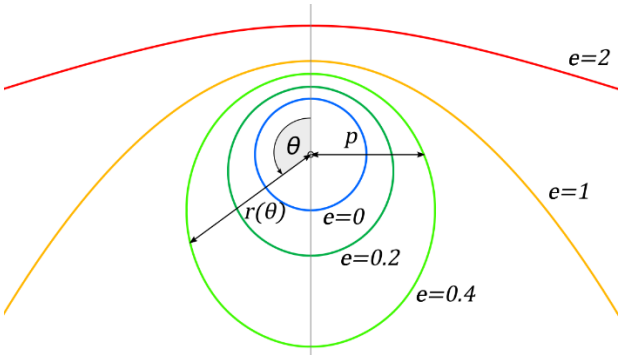

Figure 4: Geometry of conics

2.2 Equilibrium

This article considers a particular type of load, defined as follows:

Definition

A *uniform radial load* centered on a point F is a load distributed on a curve such that:

- At any point, the load direction is aligned with the line between this point and F;
- The angular pressure q (in kN/rad) from the focal point is constant. This means that the load amplitude on an elementary segment of aperture $d\theta$ is $qd\theta$ (see Figure 5).

The core of the contribution is the following proposition:

Proposition 1

A cable with conic geometry is funicular under a uniform radial load centered on a focus. The tension force in the cable is given, for a conic of eccentricity e, by:

$$T = q\sqrt{e^2 + 2e\cos\theta + 1} \qquad (2)$$

where θ is defined as in equation (1). The tension does not depend on the value of p.

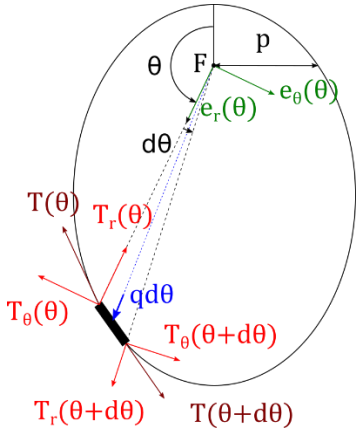

Figure 5: Equilibrium of an elementary segment of ellipse under a focal load.

Proof:

Let us consider a cable for which the reference curve is a conic given by equation (1). We introduce the local orthogonal frame polar frame $(\boldsymbol{e_r}, \boldsymbol{e_\theta})$.

Let us consider a uniform radial load emanating from a focal point: a segment of aperture $d\theta$ is subjected to a load $qd\theta\boldsymbol{e_r}$ where q is constant. We look for an admissible tension field $\boldsymbol{T}$ in the cable, of amplitude T. We decompose the tension into its radial part T_r and its orthoradial part T_θ, such that $\boldsymbol{T} = T_r\boldsymbol{e_r} + T_\theta\boldsymbol{e_\theta}$.

Notation

For functions depending on θ, we omit the mention of θ when they are evaluated at $\theta : r(\theta) = r$. When evaluating the function at a first-order angle increment $\theta + d\theta$, we write the first order development $r(\theta + d\theta) = r + dr$

Analysis

Let us look at the equilibrium of an infinitesimal portion of arch of aperture $d\theta$. The tension field must verify equilibrium of moments about the focal point. Keeping only the first order terms, this equilibrium reads:

$$r\,T_\theta = (r + dr)(T_\theta + dT_\theta)$$

$$\frac{dT_\theta}{T_\theta} = -\frac{dr}{r}$$

After integration:

$$T_\theta = \frac{C}{r}$$

Where C is a constant, homogenous to a torque.

The tension field must also verify the radial equilibrium (i.e. the equilibrium projected on $\boldsymbol{e_r}$), which reads at first order:

$$q\,d\theta + T_r(\theta + d\theta) - T_r(\theta) - T_\theta(\theta + d\theta)d\theta = 0$$

$$dT_r = (T_\theta(\theta) - q)\,d\theta$$

Using equation (1):

$$dT_r = \left(\frac{C}{p}(1 + e\cos\theta) - q\right)d\theta$$

Integrations yields:

$$T_r = T_0 + \left(\frac{C}{p} - q\right)\theta + \frac{Ce}{p}\sin\theta$$

Where T_0 is a constant. To obtain a periodic tension field, we must have $C = qp$. As a result:

$$T_r = T_0 + qe\sin\theta$$

And T_θ must be of the form $T_\theta = q(1 + e\cos\theta)$

Finally, the tension must fulfill the orthoradial equilibrium (i.e. the equilibrium projected on $\boldsymbol{e_\theta}$). Again, we discard all second order terms:

$$-T_\theta(\theta) + T_\theta(\theta + d\theta) + T_r(\theta + d\theta)d\theta = dT_\theta + T_r d\theta$$
$$= (-qe\sin\theta + T_0 + qe\sin\theta)d\theta$$

We have equilibrium if $T_0 = 0$.

Synthesis

We have found a tension field $\boldsymbol{T} = T_r\boldsymbol{e_r} + T_\theta\boldsymbol{e_\theta}$ with:

$$T_r = qe\sin\theta$$
$$T_\theta = q(1 + e\cos\theta)$$

This field is at equilibrium with the load. Let us now check that it is aligned with the cable. The cable orientation is given by the tangent vector, which is given in polar coordinates by:

$$\boldsymbol{t} = \frac{dr}{d\theta}\boldsymbol{e_r} + r\boldsymbol{e_\theta} = \frac{e\sin\theta}{1 + e\cos\theta}\, r\, \boldsymbol{e_r} + r\, \boldsymbol{e_\theta}$$

We check collinearity by calculating the cross product:

$$\|\boldsymbol{T} \wedge \boldsymbol{t}\| = \left\| qe\sin\theta\, r - \left(q(1 + e\cos\theta)\right)\frac{e\sin\theta}{1 + e\cos\theta}\, r \right\| = 0$$

The tension field is indeed aligned with the cable.

The value of the tension is given by $T^2 = T_r^2 + T_\theta^2$, such that we recover equation (2):

$$T = q\sqrt{e^2 + 2e\cos\theta + 1}$$

We remark that the square root is always well defined:

$$e^2 + 2e\cos\theta + 1 \geq\ e^2 - 2e + 1 = (e - 1)^2 \geq 0$$ ■

Case of the circle

We remark that this formula yields the classical results for tension in circles, for which $e = 0$. Indeed, we then get $T = q$. We can convert the angular load q into a normal line load μ (in kN/m) by considering at a portion of arc of length ds:

$$\mu\, ds = q\, d\theta\ \Rightarrow\ \mu = q\frac{d\theta}{ds} = q/R$$

Where R is the curvature radius. We obtain: $T = \mu R$, a well-known formula.

Hyperbolas

Hyperbolas have two branches. In formula (1), the branch closest to the focal point is reached with a positive radius, while the other branch corresponds to a negative radius (Figure 6). For this last branch, because of the negative radius, the repulsive radial force actually acts as an attracting load. The formula (2) gives a tension force which corresponds to this attracting load. If we consider the actual repulsive load, the force in equation (2) corresponds to a compression force in the bottom branch.

Discussion

The proposition is formulated for a repulsive load, which gives a conic in tension. It can also be applied to an attracting force, in which case the conic is in compression, with a compression amplitude given by (2).

This proposition implies that any non-circular conic is funicular under two different load cases, one for each focal point. Ellipses and hyperbolas have two well defined foci. The parabola has only one. However, the well-known case of a uniform vertical load can be seen as a uniform radial load emanating from a focus at infinity.

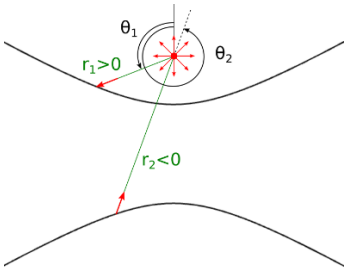

Figure 6: The two branches of a hyperbola

2.3 Force distribution

This section discusses the distribution of axial forces given by equation (2). Figure 7 shows this distribution for ellipses of various eccentricities. On a circle, a uniform radial load results in uniform tension. As the eccentricity is increased, tension at the apex closest to the focus increases, while tension at the opposite apex decreases. For a parabola, the tension is maximum at the apex, and decreases, with a limit of 0 at infinity (which corresponds to $\theta = \pi$). This behavior is opposite to the case of a uniform vertical loading, for which the axial force is minimal at the apex.

Hyperbolas are shown in Figure 8. The two branches have opposite curvature signs. As a result, the branch closer the focal point resist the load in tension, while the one further away works in compression. As the eccentricity is increased, the axial force becomes more and more uniform, but with an increasing amplitude.

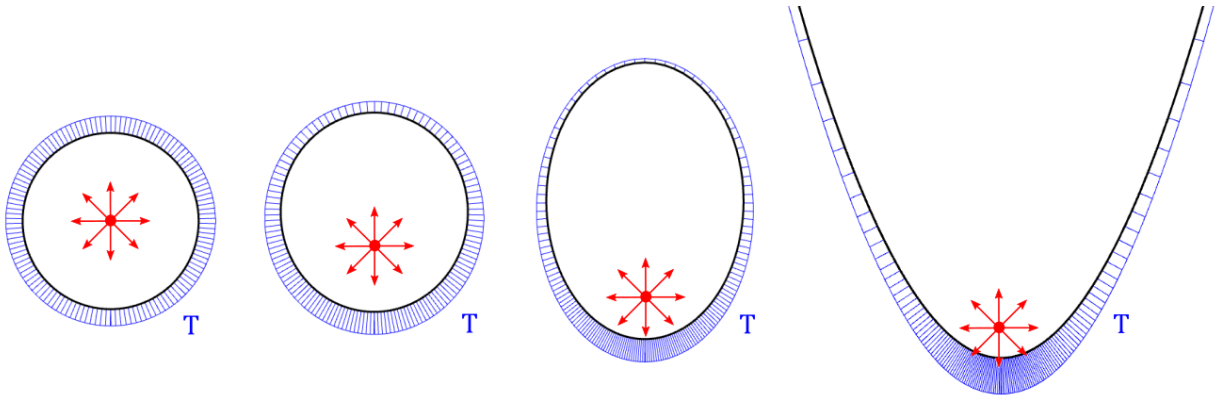

Figure 7: Distribution of tension for ellipses of various eccentricities and for a parabola

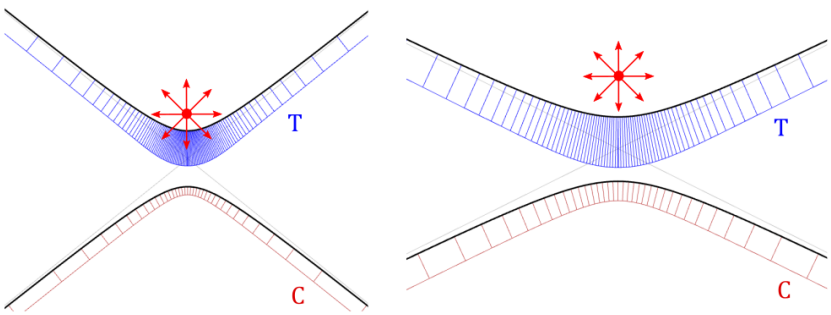

Figure 8: Distribution of tension and compression in hyperbolas with two different eccentricities

3. Discrete model

A uniform radial load is a rather abstract load case. However, it can be readily applied in a discrete form with a radial fan of cables with constant angle between two adjacent cables and constant cable tension. This discretization naturally introduces the discrete conic model of (Tsukerman 2015): As showed in Figure 9, the vertices of a discrete conic are defined as the intersection points of a smooth conic with rays emanating from a focal point with constant angle between adjacent rays. It turns out that this discrete conic model yields a simple discretization of the result of section 2:

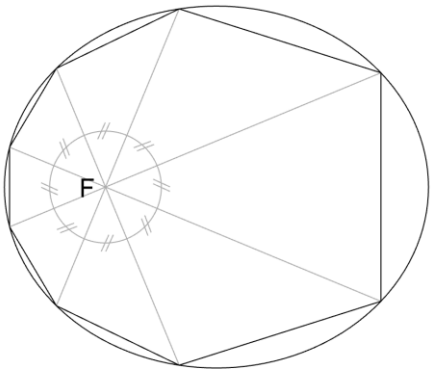

Figure 9: Discrete conic model

Proposition 2

Let us considered a polygon with vertices V_i inscribed in an conic of focus F, $F°$, such that the angles $\widehat{V_iFV_{i+1}}$ are constant (Figure 10). The polygon $V_1 \dots V_n$ is then funicular for a uniform tension applied in cables V_iF (proper support still needs to be provided at the polygon extremities if it not closed).

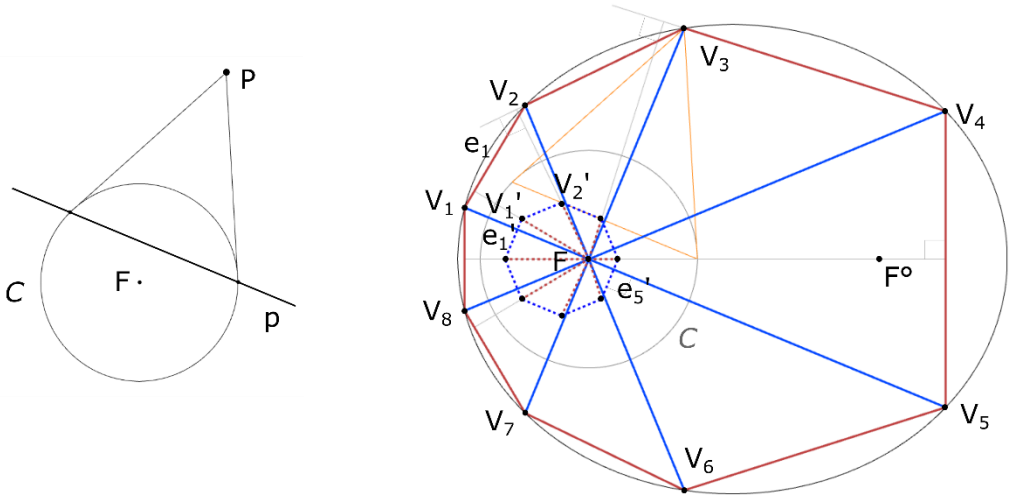

Figure 10: Left : Reciprocal duality. Right: a discrete conic (solid red)

Proof:

We base our proof on the approach and results of (Tsukerman 2015). We use the concept of reciprocal duality with respect to a circle. Referring to Figure 10 (left), a reciprocal duality transforms a point P into a line p, and reciprocally the line p into the point P, such that the line p is the one passing through the tangency points of the tangents to the circle passing through P. The construction is also defined via inversions if the point is insider the circle – see (Tsukerman 2015). An important aspect is that, in any

case, the line p is perpendicular to the line (PF). We define the reciprocal duality d with respect to a circle C centered at the focus F of the conic – the radius of the circle is arbitrary. As shown by Tsukerman, the reciprocal dual lines of the vertices V_i define the edges of a regular polygon $V_1' \dots V_n'$, in which V_j' is the reciprocal dual of the edge e_j of the discrete conic. The construction of edge e_3' from V_3 is shown in orange.

By construction: the line (FV_i) is perpendicular to e_i' for any i, and the edge e_j is perpendicular to the line FV_j' for any j. Hence, up to rotation of 90°, the polygon $V_1' \dots V_n'$ and the segments FV_j' form a valid reciprocal force diagram. The axial force in a ray FV_i is represented by the length of the edge e_i'. Since $V_1' \dots V_n'$ is a regular polygon, the axial force in the rays FV_i is hence constant. ■

Remark 1: In a more general way, the application of reciprocal dualities for structural design is explored in (Konstantatou *et al.* 2018)

Remark 2: As proven in (Micheletti 2008), the reciprocal diagram of a self-stressed structure also corresponds to the geometry of a self-stressed system. Consequently, the regular polygon $V_1' \dots V_n'$ with the rays FV_j' form together a self-stressed structure.

4. Design applications

Radial loads are not encountered in nature: self-weight, snow, or wind loads rarely correspond to this distribution. However, as discussed in section 3, they do correspond to the tension induced by radial cables with constant tension and constant angle, such as the spokes of a bike wheel. As detailed in section 1, the design of prestressed systems is usually a complex task, which requires iterative numerical analysis. The result showed in sections 2 and 3 allows to design the equilibrium state of a certain family of self-stressed structures without any computational effort.

A first example is the elliptical arch showed in Figure 1. It is funicular under a prestressing imposed by cables emanating from a focal point – with constant angle between the cables and constant cable tension. Compression forces in the arch can be directly estimated from equation (2). The fact that cable tension is constant can simplify the prestressing procedure: If cables are connected to a circular cable, a simple way to insure that the radial tension is uniform is to check that the center cable is circular.

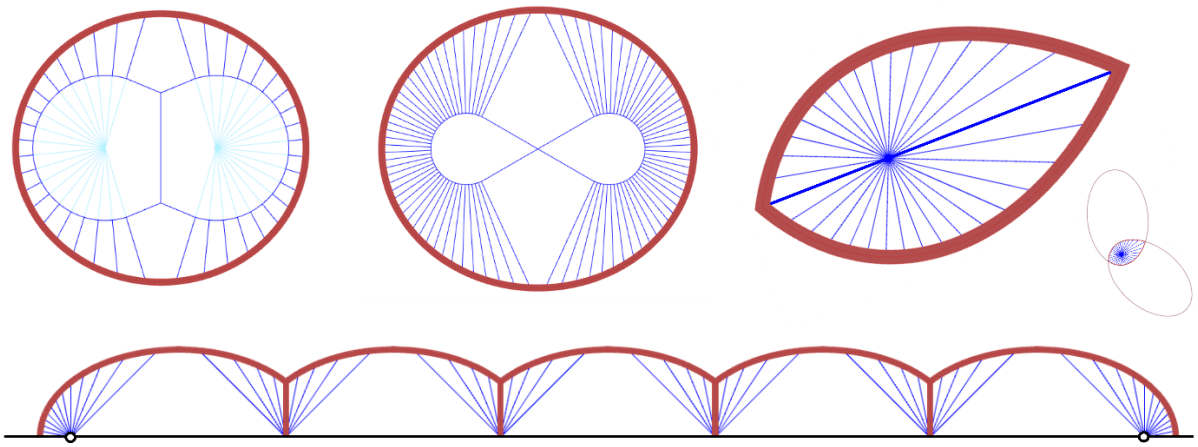

Figure 11: Self-stressed funicular structures composed of elliptical arches.
Red: Compression elements. Dark blue: Tension elements. Black: Supports

The fact that ellipses are funicular under two different load cases is used in Figure 11 (top left) to design a funicular arch prestressed from the two focal points. We use the fact that the two loads cases (one for each

focus) give the same axial force at the apex: this allows to pretension the left half from the left focus, and the right half from the right focus. An intermediate vertical cable is necessary to close the circular cables. For the sole purpose of structural delight, this geometry can be adjusted such that this vertical cable is not necessary – closing of cables being realized as an 8-loop (top middle image).

Arches from ellipses sharing a common focus but with axes at different angles can be joined as shown in the top right image. The two arches press against each other with the same force because of the symmetry. At the junction of the two arches, because of the lateral push of the arches, the cable takes more tension than its neighbours (it is hence depicted with a thicker blue line). Remarkably, this lateral push has the same value at both ends, despite their different slope. This is due to the fact that the projected tension on a radial axis (T_r) as a π-periodic amplitude. This allows the structure to be self-stressed without support. The bottom picture shows how ellipses can be joined in series. Bottom of piles are located at focal points. Only the extreme two foci need to withstand lateral loads. An interesting aspect of the proposition is that these structures were designed with simple geometrical rules.

The proposition also implies that parabolas are funicular for two load cases: the well-known uniform vertical force, and a radial load emanating from their focal point. The parabolic arch showed in Figure 12 (top-left) is for example pretensioned radially from the focus. This allows the arch to resist live loads. As in Figure 1, radial cables are connected to a circular cable, which allows circulation under the arch.

Figure 12 (bottom left) shows a hyperbolic arch, prestressed by a hyperbolic cable. The two hyperbolas have a common focal point. Figure 12 (right) shows an arch composed of four arcs of hyperbola, with C1 junctions. Each arc is funicularly prestressed by radial cables emanating from its focus. Thanks to the symmetry, the resultant forces at each cable fan can be balanced by the resultant at the opposite corner via a diagonal cable.

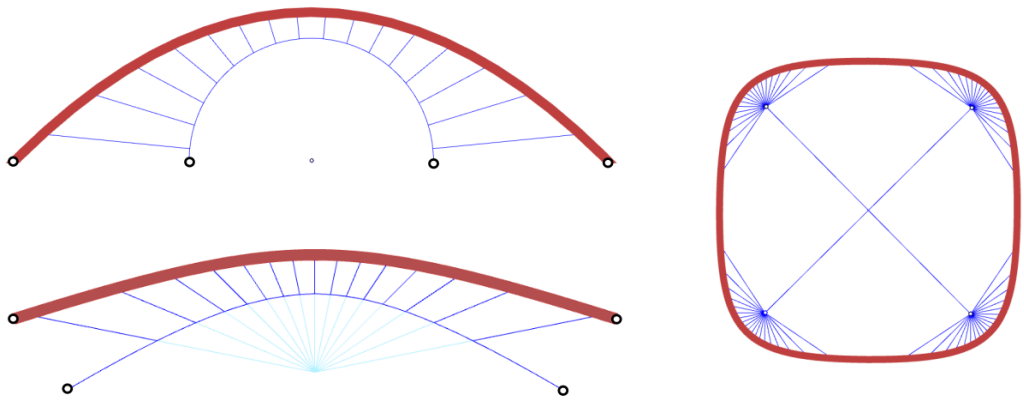

Figure 12: Self-stressed funicular structures composed of parabolas, hyperbolas and circles. Red: Compression elements. Dark blue: Tension elements. Black: Supports

Tensegrity

The proposition can also be used to design non-planar self-stressed structures. Figure 13 shows two roof structures based on the tensegrity Geiger system, a typology for example used in the Olympic Fencing stadium in Seoul, Korea (1986) and in the Georgia dome shown in Figure 2. The left one is based on two ellipses with a common focus. The inner ellipse is offset vertically twice (once up, once down), and joined by vertical struts. Radial cables from the common focus are drawn with equal angles. This structure is funicular provided that the tension in the radial cables, once projected on the horizontal plane, is constant (as shown in the inset in Figure 13 left). The vertical equilibrium is guaranteed by the symmetry.

The right pictures on Figure 13 shows a more complex arrangement, based on three ellipses. Each ellipse shares a focus with the adjacent ellipses, but they do not have the same axis orientation. Contrary to the left structure, radial cables are spaced such that their anchor points on the outer compression ring are

equidistant. In order to obtain an equivalent smooth uniform radial load acting on the compression ring, the tension in the radial cables must be inversely proportional to the angle between the two adjacent spokes – tensions are hence not constant anymore. For the middle ellipse to remain in tension, the tension in the outer axial cables must be significantly higher than in the radial cables spanning between the small and the medium ellipse.

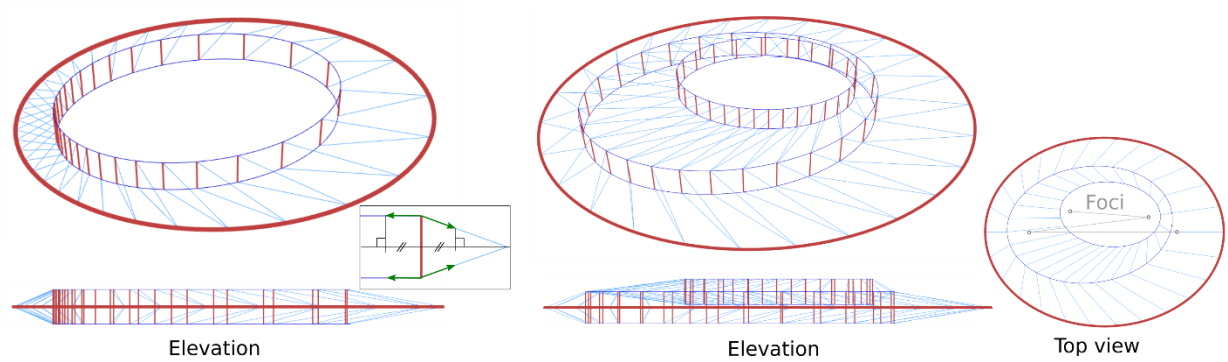

Figure 13: Tensegrity Geiger roof structures generated from conics sharing a focus. Red: compression elements. Blue: tension elements.

Line of thrust

Proposition 2 allows to construct the thrust line representing the funicular equilibrium of a conic. It is of particular interest for the design of masonry arches, as simple rules can be applied to insure stability of the vaults (Heyman 1997). In particular, one can check that the thrust line remains within the middle third of the section under main load case.

This is demonstrated on the parabolic arch showed in Figure 14. A parabola is discretized by intersecting it with cables emanating from the focus at constant angles. This yields the red parabolic polyline (the thrust line), which is funicular for a constant tension from the cables. The initial parabola is then offset to create the geometry of masonry blocs of constant length. The arch is tied and simply supported on two columns. The vertical force which is necessary to balance the tension in the cable fan is symbolized by a hanging block. A system of pulleys is schematically suggested to insure that the tension in the eight top cables is constant.

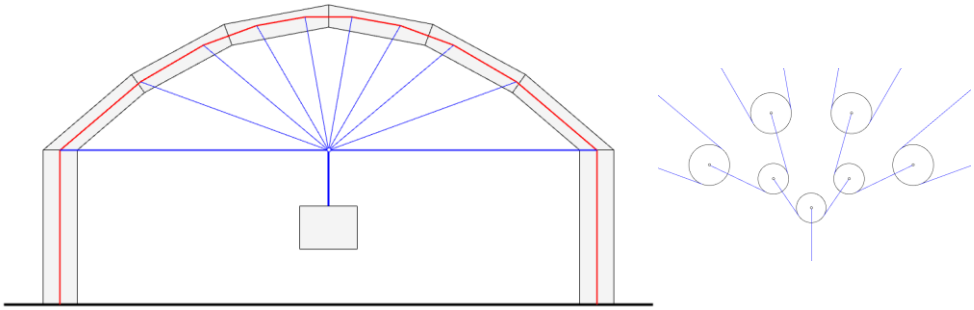

Figure 14: A self-stressed parabolic masonry arch, and a system of pulleys that insures that cables have equal tension

Analogy with optics

The proposed result evocates strongly the optical properties of mirrors shaped as conics. Inspired by this analogy, Figure 15 proposes a system to convert a radial fan of cables into an array of parallel cables. The junction can be realized by a funicular arc of parabola. Radial cables have constant tension and constant angle, parallel ones have constant spacing and constant tension (different from the radial cables tension).

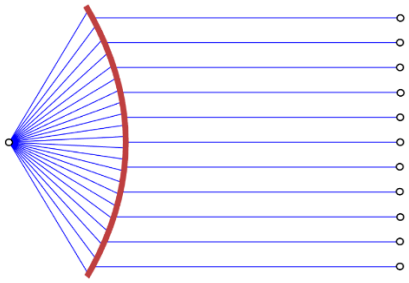

Figure 15: Analogy with optics: reorienting radial cables into a parallel array with a parabolic funicular arch

5. Discussion

This section discusses the scope and limitations of the present work and gives suggestions for future research.

Stability

We have considered in this article only the axial forces under a prestressing load case. This information gives a lower-bound on the cross-sectional area of the components. However, for a final design, stability must be accounted for in the design of the compression elements.

Firstly, one needs to take into account for varying load conditions. In particular, one would need to obtain a proper bending resistance. For a masonry arch, a sufficient thickness would also be needed to avoid the apparition of a mechanism between the blocks.

Secondly, buckling should also be considered. In this respect, similarly to the case of the circular arc subjected to uniform pressure treated in (Timoshenko and Gere 1961), proposition 1 might be used to obtain analytical formulas for the buckling of conic-shaped arches. However, the result is likely to involve elliptic integrals.

Use in numerical solvers

Another path to pursue would be to use the proposed analytical formula as an initialization for numerical form-finding methods, a point which might help or speed-up convergence.

Design abacus

In order to design by hand conics and combinations of conics such as the ones showed in section 4, it is useful to have a chart of confocal ellipses and hyperbolas, such as the one showed in Figure 16. Rays with constant angle emanating from a focus are shown, such than one can visualize in one single figure a wide variety of self-stressed structures. The potential of this method could be explored in future work or in student workshops.

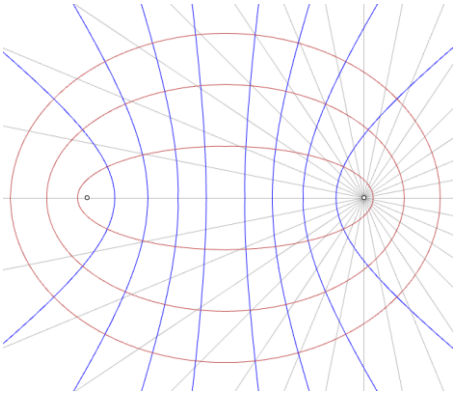

Figure 16: A chart of confocal ellipses and hyperbolas

6. Conclusion

Conics have a fascinating array of geometrical properties and physical applications. This article adds a mechanical one to the list: Conics are funicular for a uniform radial load emanating from a focal point. This result can be used to design a wide array of self-stressed funicular systems. These can be obtained by hand, without calculation, which makes the result useful at conceptual design phases.

Declarations

Funding
This work is supported by Labex MMCD (http://mmcd.univ-parisest.fr/).

Conflict of interest/Competing interests
The authors have no conflict of interest to disclose.

Availability of data and material
Not applicable

Code availability
Not applicable

References

Alexakis, H., Makris, N. (2013) 'Minimum thickness of elliptical masonry arches', *Acta Mechanica*, 224, 2977–2991.

Block, P. (2009) *Thrust Network Analysis. Exploring Three-Dimensional Equilibrium*.

Cremona, L. (1890) *Graphical Statics: Two Treatises on the Graphical Calculus and Reciprocal Figures in Graphical Statics*, Claredon Press.

Dennis, N. (1994) 'On the formation of funicular curves', *International Journal of Mechanical Science*, 36(3), 183–188.

Fivet, C. (2016) 'Projective transformations of structural equilibrium', *International Journal of Space Structures*, 31(2–4), 135–146.

Fung, T.C. (2003) 'Shapes of submerged funicular arches.', *Journal of engineering mechanics*, 129(1), 120–125.

Gavin, H.P., Reilly, K.J. (2000) 'Submerged funicular arches', *Journal of Structural Engineering*, 126(May), 627–629.

Glaeser, G., Stachel, H., Odehnal, B. (2016) *The Universe of Conics*, Springer Spektrum.

Heyman, J. (1997) *The Stone Skeleton: Structural Engineering of Masonry Architecture*, Cambridge University Press.

Hill, R.D., Rozvany, G.I.N., Ming, W.C., Hwa, L.K. (1979) 'Optimization , Spanning Capacity , and Cost Sensitivity of Fully Stressed Arches', *Journal of Structural Mechanics*, 7(4), 375–410.

Konstantatou, M., D'Acunto, P., McRobie, A. (2018) 'Polarities in structural analysis and design: n-dimensional graphic statics and structural transformations', *International Journal of Solids and Structures*, 152–153(July), 272–293, available: https://doi.org/10.1016/j.ijsolstr.2018.07.003.

Lee, J., Fivet, C., Mueller, C. (2015) 'Grammar-based generation of equilibrium structures through graphic statics', in *Proceedings of the International Association for Shell and Spatial Structures Symposium (IASS)*.

Liu, Y., Snyder, J., Wang, W. (2013) 'Computing Self-Supporting Surfaces by Regular Triangulation', *ACM*

Transactions on Graphics, 32(4).

Micheletti, A. (2008) 'On generalized reciprocal diagrams for self-stressed frameworks', *International Journal of Space Structures*, 23(3), 153–166.

Ohlbrock, P.O., Schwartz, J. (2016) 'Combinatorial equilibrium modeling', *International Journal of Space Structures*, 31(2–4), 177–189.

Otter, J., Cassel, A., Hobbs, R. (1966) 'Dynamic relaxation', in *Proceedings of the Institution of Civil Engineers*, 633–656.

Rankine, W.J.M. (1858) *A Manual of Applied Mechanics*, London; Glasgow: Marion R Griffin & Co.

Schek, H.J. (1974) 'The force density method for form finding and computation of general networks', *Computer Methods in Applied Mechanics and Engineering*, 3(1), 115–134.

Schober, H. (2015) *Transparent Shells: Form, Topology, Structure*, Ernst & Sohn.

Simpson, A., Tabarrok, B. (1976) 'Chain subjected to uniform fluid flow in a horizontal plane', *International Journal of Mechanical Science*, 18, 91–94.

Tamai, H. (2019) 'Geometric approach to form finding of a spoke wheel system: Mathematical explanations', in *Proceedings of the IASS Annual Symposium*, 692–699.

Tellier, X., Douthe, C., Hauswirth, L., Baverel, O. (2020) 'Linear-Weingarten membranes with funicular boundaries', *Structural Concrete*, 1–14.

Tellier, X., Hauswirth, L., Douthe, C., Baverel, O. (2018) 'Discrete CMC surfaces for doubly-curved building envelopes', in *Advances in Architectural Geometry*, 166–193.

Timoshenko, S.P., Gere, J.M. (1961) *Theory of Elastic Stability*, McGraw-Hill Books Company, New York and London.

Todisco, L., Corres, H. (2018) 'New opportunities for the conceptual design of material-efficient antifunicular structures', *Hormigón y Acero*, 69(284), 83–88.

Tsukerman, E. (2015) 'Discrete Conics as Distinguished Projective Images of Regular Polygons', *Discrete and Computational Geometry*, 53(4), 691–702, available: http://dx.doi.org/10.1007/s00454-015-9669-y.

Vouga, E., Mathias, H., Wallner, J., Pottmann, H. (2012) 'Design of Self-supporting Surfaces', *ACM Trans. Graph.*, 31(4).

Wang, C.M., Wang, C.Y. (2002) 'Funicular Shapes for Submerged Arches', *Journal of Structural Engineering*, 128(2), 266–270.

Wang, C.Y., Wang, C.M. (2015) 'Closed-form solutions for funicular cables and arches', *Acta Mechanica*, 2226, 1641–1645.